FOI

IED-Logistics report, December 2011

Status report of demonstrator

MARIA AXELSSON, IDA JOHANSSON, PETRA KÄCK,
OLA NORBERG, MARKUS NORDBERG

FOI-R--3346-SE Technical report
ISSN 1650-1942 December 2011

Defence & Security, Systems and Technology

Maria Axelsson, Ida Johansson, Petra Käck, Ola Norberg, Markus Nordberg

IED-Logistics report, December 2011

Status report of demonstrator

Titel	Rapport för IED-Logistics, december 2011-Status rapport för demonstrator
Title	IED-Logistics report, December 2011-Status report of demonstrator
Rapportnr/Report no	FOI-R--3346-SE
Rapporttyp/ Report Type	Teknisk rapport / Technical report
Sidor/Pages	30 p
Månad/Month	December/December
Utgivningsår/Year	2011
ISSN	1650-1942
Kund/Customer	Försvarsmakten
Projektnr/Project no	E26454
Godkänd av/Approved by	Sten E. Nyholm

FOI, Totalförsvarets Forskningsinstitut
Avdelningen för Försvars- och säkerhetssystem

164 90 Stockholm

FOI, Swedish Defence Research Agency
Defence & Security, Systems and Technology

SE-164 90 Stockholm

Sammanfattning

Hemmagjorda sprängladdningar (IED:er, från engelskans 'improvised explosive device') utgör ett stort hot mot såväl det civila samhället som militära operationer och det finns ett behov av att detektera och identifiera sådana sprängladdningar där de förekommer i dag. Ett sätt är att spåra upp och angripa det nätverk som producerar, hanterar och placerar ut laddningarna. Vid hantering av sprängämnen blir det ofta spårpartiklar kvar och syftet med det här projektet är att vidareutveckla ett sensorsystem som kan finna dessa spårpartiklar. Systemet bygger på hyperspektral avbildande Ramanspektroskopi och innehåller en UV-laser; det kommer att bli mobilt och lämpligt för användning i fält.

Denna rapport tar upp det pågående arbetet att utveckla ett avbildande UV-Raman system.

Delar av arbetet har gjorts hand i hand med ett annat projekt som heter CEREX (Collaborative Effort for Raman Explosive detection). Projektet, i vilket det avbildande Ramansystemet är utvecklat, är finansierat av Myndigheten för samhällsskydd och beredskap.

Ett grafiskt användargränssnitt håller på att utvecklas för att få ett användarvänligt system. Användargränssnittet kommer att visa en vidvinkelbild och en förstorad bild av målet och några kontrollknappar.

För att kunna identifiera målen håller tre typer av metoder för spektra klassificering att undersökas. Som ett första steg, har antalet Ramanskift att mätas på minskats genom "feature selection". Preliminära resultat visar att vid mätning på svavel (S), ammoniumnitrat (AN), 2,4-dinitrotouluene (DNT) och 2,4,6-trinitrotouluene (TNT) 8-10 skift är nog för att inte tappa precision i beräkningarna.

Bra Ramanspektra har blivit uppmätta från polytetrafluoroethylene (PTFE), kaliumklorat (PC), AN, ureanitrat (UN) and cyclotrimethylenetrinitramine (RDX) vid 355 nm laservåglängd.

Dessutom, genom att använda en OPO-laser och avstämbara filter, Ramanspektra från ovan ämnen har blivit mätta med laservåglängd mellan 320-360 nm. För de flesta proven minskar Ramansignalen kraftigt när man går mot kortare våglängder.

Nyckelord: UV-Raman, multispectral avbildning, IED, detektion

Summary

Improvised explosive devices, IEDs, are a common threat to the civilian society and military operations, therefore there is a need to detect and identify such explosive charges in real environments. One way is to find and attack the network behind the production, handling and placement of the charges. The handling of explosive material often leaves trace particles behind and the aim in this project is to further develop a sensor system for finding these trace particles. The system will be based on multispectral imaging Raman spectroscopy, utilising a UV laser; it will be mobile and suitable for field applications.

This report shows the ongoing work on developing an imaging UV-Raman system.

Parts of the work have been made hand in hand with another project called the CEREX project (Collaborative Effort for Raman Explosive detection). The project, in which the imaging Raman system has been developed, is funded by the Swedish Civil Contingencies Agency.

A graphical user interface (GUI) is under development to give a user friendly control system. The GUI will show a near- and a far-field view of the target together with some control buttons.

In order to identify the targets, three different types of methods for spectra classification is been investigated; a) direct fitting, b) classification methods and c) subspace methods. A first step has been, to reduce the number of Raman shifts to measure at by feature selection. Preliminary results shows that for sulfur (S), ammonium nitrate (AN), 2,4-dinitrotouluene (DNT) and 2,4,6-trinitrotouluene (TNT) 8-10 shifts are enough when using least square fitting.

Good Raman spectra from polytetrafluoroethylene (PTFE), potassium chlorate (PC), AN, urea nitrate (UN) and cyclotrimethylenetrinitramine (RDX) have been recorded at 355 nm laser wavelengths.

Also by using a tunable OPO-laser and a tunable notch filter, Raman spectra of the same substances have been recorded in the 320-360 nm laser wavelength range. For most targets the measured Raman signal decreases considerably towards shorter wavelengths.

Keywords: UV-Raman, multispectral imaging, IED, detection

Table of Contents

1 Introduction

Improvised explosive devices, IEDs, are a common and a growing threat to the civilian society as well as to military operations. Detecting and identifying explosive charges and IEDs in real environments is a very challenging and in many cases hazardous task.
One way to tackle the IED problem is to find and attack the network behind the production, handling and placement of the charges. The handling of explosive material often leaves trace particles behind, for example on cars or outside the production site buildings. Within the project IED-Logistics, the aim is to further develop a sensor for detection and identification of these traces.

FOI has previously reported [1-4] Raman spectroscopy as a good method for stand-off detection of explosives in bulk amounts. The technique can be used in different environmental conditions, such as rain, snowfall and sunshine. It can also be applied at distances up to several hundreds of meters, and has been tested on explosives such as triacetonetriperoxide (TATP), hexamethylenetri-peroxidediamine (HMTD), hydrogenperoxide (H_2O_2), methylethylketoneperoxide (MEKP), nitromethane (NM), 2,4-dinitrotoulene (DNT), 2,4,6-trinitrotoluen (TNT) and ammonium nitrate (AN).

In this project the detection system will be based on multispectral imaging Raman spectroscopy [5, 6], and the project will result in a mobile detector prototype, suitable for field applications, which can be used to examine non-moving targets (such as vehicles, clothing, luggage, buildings et cetera.).

Parts of the work have been made hand in hand with another project called the CEREX project (Collaborative Effort for Raman Explosive detection). The project, in which the imaging Raman system has been developed, is funded by the Swedish Civil Contingencies Agency. The system developed in CEREX uses a green 532 nm laser and is in the present stage capable of detecting and identifying particles less than 100 µm at 10 m distance [7].

In this project a UV-laser will be used. The main reason why this region is interesting is that UV light, which is outside the visible spectral region, is much less hazardous to the eye, since these wavelengths are not focused by the lens of the human eye onto the retina. It would therefore be possible to construct a UV Raman system that is eye safe. Another important advantage of using UV light is that detection can be made without drawing attention, even without anyone knowing, since the probe light is invisible.

Another advantage in using UV-light is that the Raman signal intensity scales as $1/\lambda^4$, where λ is the wavelength of irradiation. This makes the Raman signal increase at shorter laser wavelengths. In addition, many explosives undergo resonance enhancement in the UV. This happens when the laser wavelength is close to an electronic transition within the molecule and can give rise to enhancements of certain Raman lines (those coupled to the electronic transition).

Materials that appear transparent to the eye, such as glass and water, are also transparent to light at 355 nm, which makes it possible to perform detection during rain and through windows. 355 nm is also the third harmonic wavelength of Nd:YAG lasers, which makes it a suitable wavelength for the Raman system since Nd:YAG lasers are well suited for explosives detection, being compact, with short pulses and high pulse energy.

2 Software system design

To be able to set up and control the system hardware an easy to use Graphical User Interface (GUI) is being developed.

2.1 Main GUI functionality

The GUI is divided into a number of pages, one main page handling actual aiming (white light images from the two CCD-cameras) and measuring (start/stop measuring buttons), and sub-pages to set different parameters of the hardware. Common for all pages is a view with the current hardware status.

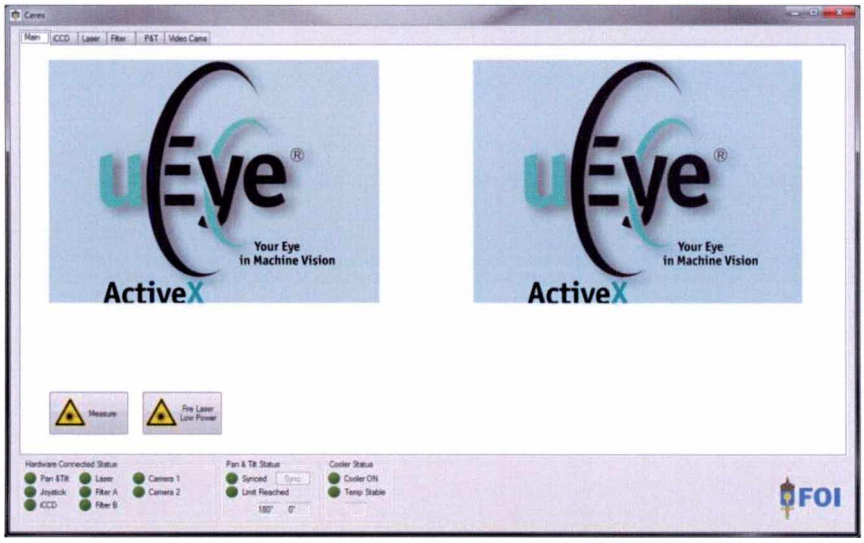

Figure 1 Main page of the GUI, the page that is used for normal operation.

In the main view, Figure 1, the operator can read the connection status of:

- Pan&Tilt head
- Joystick
- ICCD camera
- Laser
- Filters
- CCD cameras including live images from the two cameras.

When the "Pan & Tilt", "Joystick" and "Synced" lamps are green it is possible to move the Pan&Tilt with the joystick.

When "Camera 1" and "Camera 2" lamps are green the near (inline) and far video camera views are displayed in the two main video camera windows.

When "ICCD", "Laser", "Filter A" and "Filter B" lamps are green it is possible to launch a measurement.

In Figure 2 - Figure 6 advanced settings for the ICCD, laser, filter Pan&Tilt-head, and the video cameras can be found.

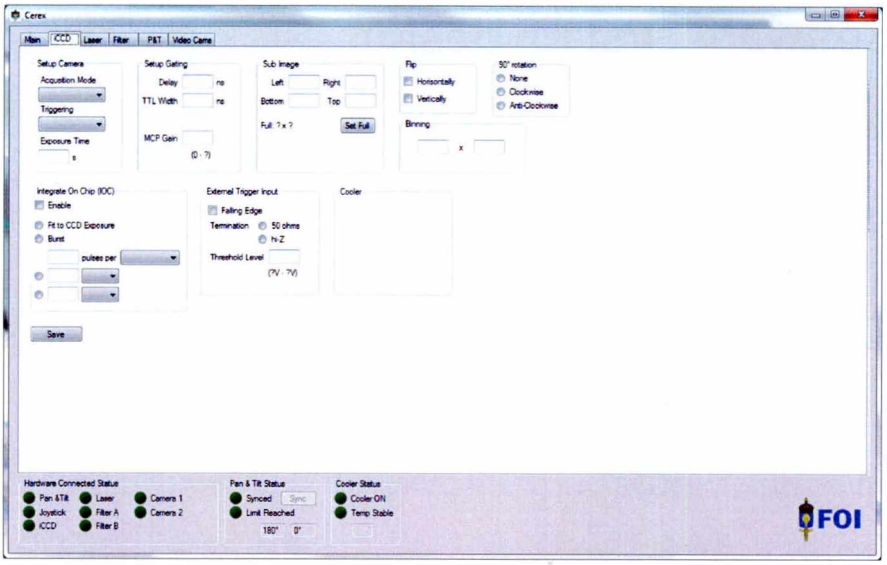

Figure 2 iCCD-page of the GUI, the page is used for setting advanced parameters of the iCCD-camera.

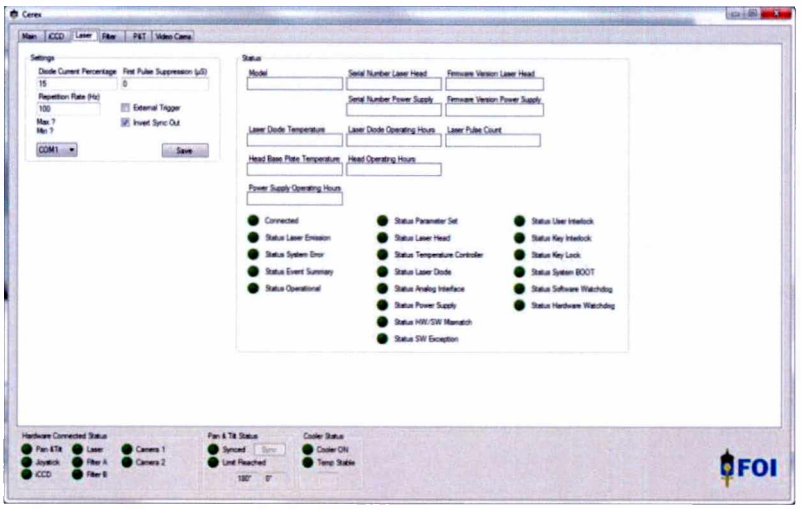

Figure 3 Laser-page of the GUI, the page is used for setting advanced parameters of the laser.

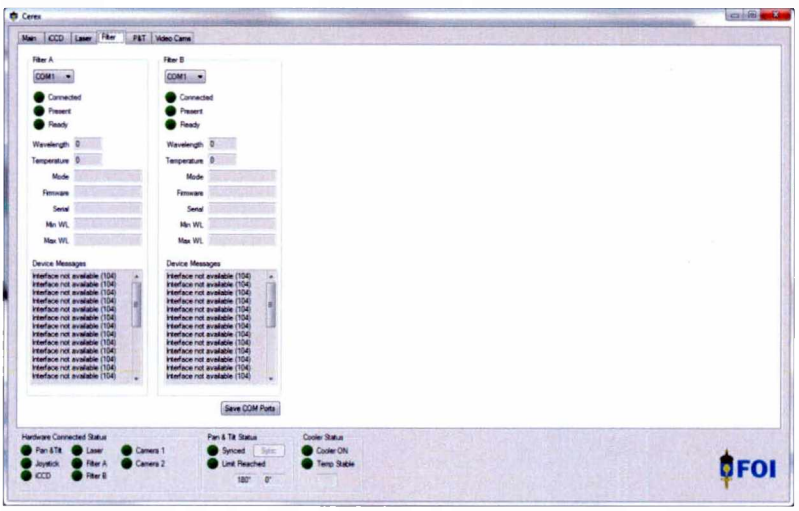

Figure 4 Filter-page of the GUI, the page is used for setting advanced parameters of the filter.

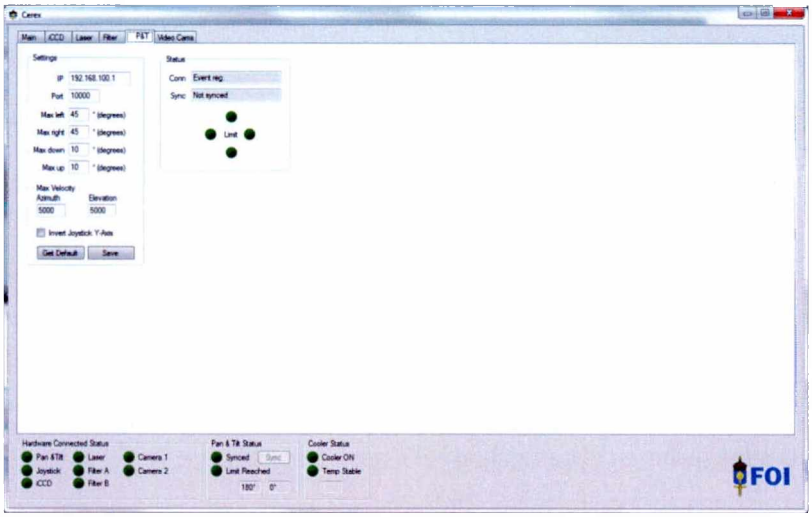

Figure 5 P&T-page of the GUI, the page is used for setting advanced parameters of the pan and tilt head.

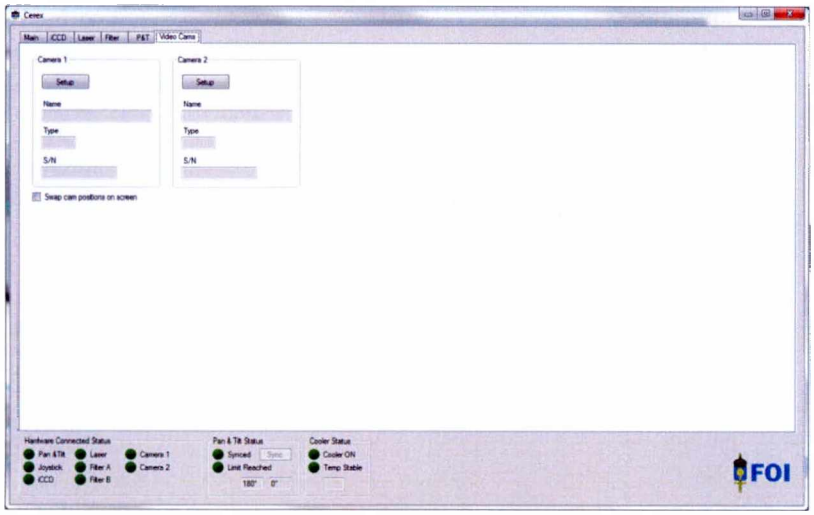

Figure 6 Video Cams-page of the GUI, the page is used for setting advanced parameters of the video cameras.

3 Spectrum classification

Methods for spectrum classification can be applied to detect explosive substances in a measurement. Fast analysis of measurements is desired as well as a short measurement time. The measurement time can be reduced by measuring at a smaller number of shifts. Methods for feature selection, i.e., selection of wave numbers relevant for analysis, are therefore investigated to make it possible to reduce the number of shifts. Methods for spectrum classification and feature selection are developed in the project and an outline of the ongoing work and some preliminary results are described here.

3.1 Methods

Two methods for spectrum classification have been proposed:

- *Least squares*. Least squares fitting of the measured spectrum in a pixel to the reference spectra from a set of substances and a constant spectrum. The recognized substance in the pixel is given by the maximum coefficient.
- *Correlation*. In this method the reference spectra are correlated with the measured spectrum in a pixel. The substance with the maximum correlation above 0.5 is used as the recognized substance. If no substance is detected the pixel is classified as background.

In the ongoing work we are investigating the accuracy of these two methods, possible improvements of the methods, and other approaches. We are currently investigating three types of methods:

- Direct fitting or regression methods such as least squares.
- Classification methods using for example k-nearest neighbors and Support Vector Machines.
- Subspace methods such as creating a new basis which describes each substance and projecting the measured spectrum onto this basis. The fit is measured using the residual.

All suggested methods use supervised learning with known spectra from measurements with the same sensor or previously measured reference spectra. In addition to the method development we have started to investigate methods for feature selection and also the impact of adding substances to the reference database.

3.2 Feature selection

Preliminary results on feature selection show that it can be possible to reduce the number of measured shifts while maintaining the classification accuracy. In this experiment a sample with four substances (sulfur, DNT, ammonium nitrate, and TNT) was used in the analysis. Each substance was marked and divided into a training set and an evaluation set. The separations between each substance/class and all other substances and background were measured for each shift in a training set. A score for each class and shift was obtained according to

$$f(i)=\frac{\left(\bar{x}_i^{(+)}-\bar{x}_i\right)^2+\left(\bar{x}_i^{(-)}-\bar{x}_i\right)^2}{\frac{1}{n_+-1}\sum_{k=1}^{n+}\left(x_{k,i}^{(+)}-\bar{x}_i^{(+)}\right)^2+\frac{1}{n_--1}\sum_{k=1}^{n-}\left(x_{k,i}^{(-)}-\bar{x}_i^{(-)}\right)^2},$$

where + indicates the set of positive features, - the set of negative features, and no indication is the whole set. The highest score values were then used to rank the importance of the 23 available shifts. The spectra in the five evaluation areas were classified using

reduced sets of shifts and the least squares approach. Figure 7 shows the accuracy of the reduced classifiers on the five evaluation regions. Figure 8 shows the corresponding classification results in the entire image for 5, 6, 7, 8, 9, and all 23 shifts. As can be seen in both Figure 7 and Figure 8 it is possible to reduce the number of features while maintaining the accuracy. This needs further investigation to see if the result is valid also for other data sets and in the case with more substances available in the database. It is likely that at least one peak must be measured for each substance which is to be detected.

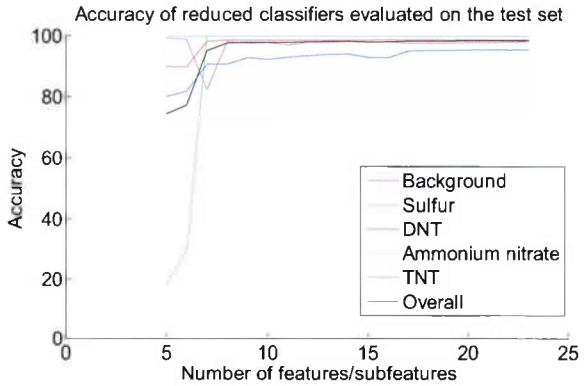

Figure 7 Accuracy of reduced classifiers using least squares analysis on an evaluation set (different from the set used to select the features.).

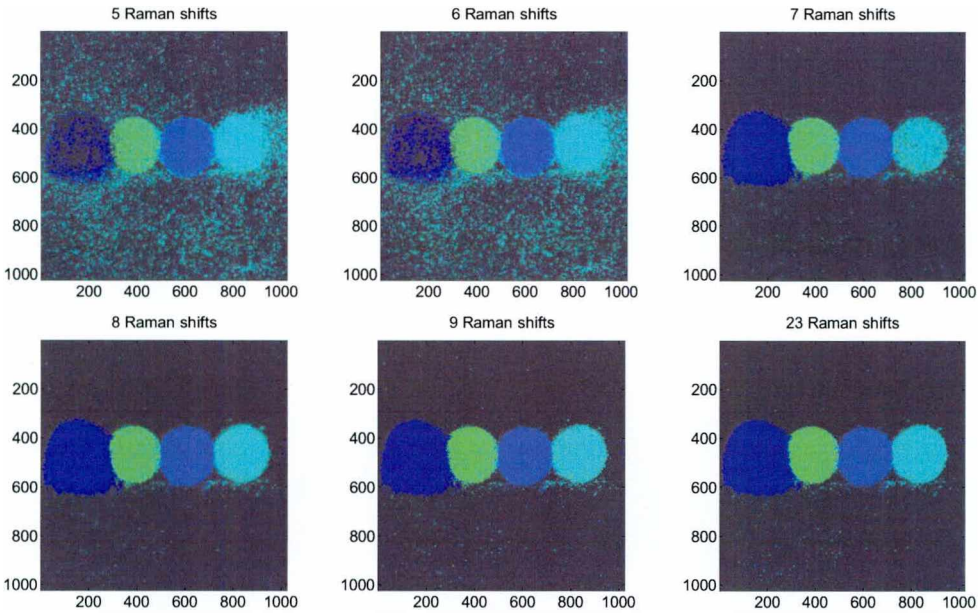

Figure 8 Analysis of four substances (sulfur, DNT, ammonium nitrate, and TNT) using a least squares approach and a reduced number of measured shifts.

3.3 New measurements and analysis

A series of measurements with eight substances have been collected with the demonstration system. The series consists of six test plates with all eight substances on each plate. Each plate was measured two times and rotated in between the measurements. A measurement consists of a series of images where an image is obtained at a given wave number. For method development purposes images were recorded at 52 wave numbers. This makes it possible to evaluate methods for feature selection. Each image in the series was exposed 1 second and gain was set to 4000 on the CCD-array. The camera was cooled to -30 °C. This gives images with low noise suitable for method evaluation. Reference

spectra from all eight substances were also recorded with a Bruker IFS 55 with a FRA 106 Raman module that uses a Nd:YAG laser at 1064 nm. Figure 9 (Left) shows an example of a white light image of one of the six test plates and Figure 9 (Right) shows a measured image at 1043 cm^{-1}. Each image measured at a specific wave number is 1024×1024 pixels. The resulting measurement is a data cube with 1024×1024×52 pixels with two spatial and one spectral dimension.

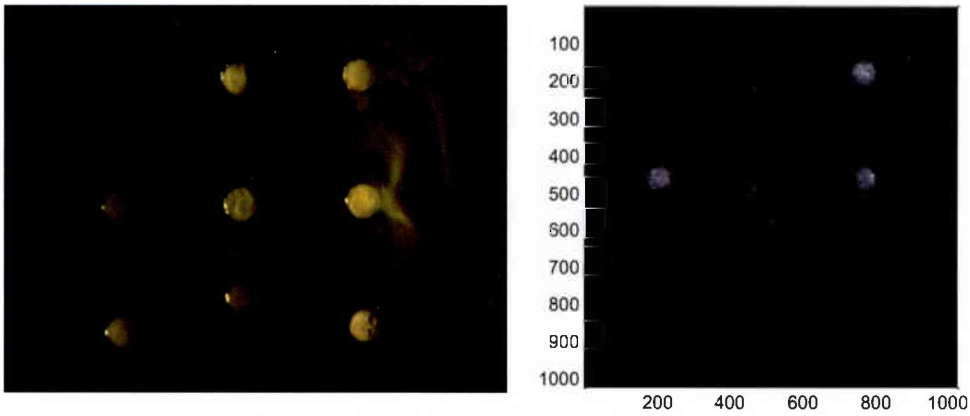

Figure 9 (Left) White light image of the test plate. (Right) Measured image showing Raman shift measured at 1043 cm^{-1}.

Preliminary analysis of the new measurement series shows that some substances have a different appearance than expected. Not all substances show the expected peaks at specific shifts. However, it has been possible to perform analysis also on this data. Figure 10 shows a set of example spectra from one of the images. The y-axis shows the 52 spectral bands and along the x-axis all pixels in seven regions (one for each substance) have been stacked. The green line is a scaled version of the pixel class label which indicates the different regions. A peak in the spectrum, which can be used for classification, will show up in the image as a line across all pixels for that substance and shift. As can be seen in the figure, classification will be more difficult for at least three of the substances (PETN, RDX, and urea nitrate) with almost even intensity and only weak lines.

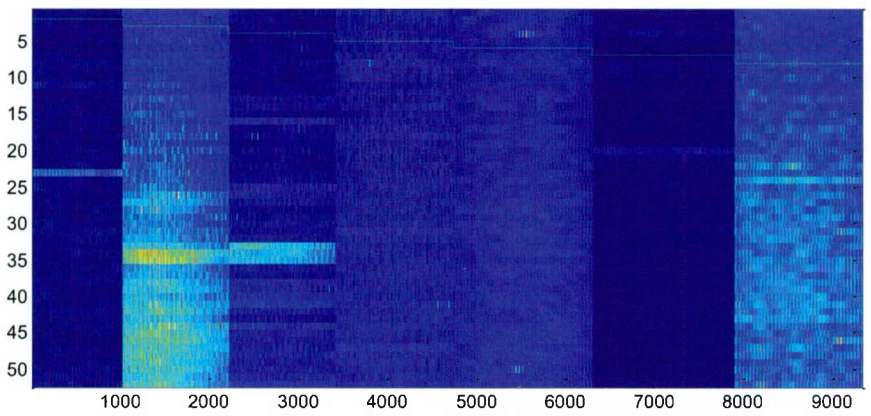

Figure 10 Example of the spectral content in seven regions corresponding to seven substances in an image. The x-axis shows the 52 spectral bands and the pixels in seven image regions are stacked along the y-axis. The regions are ordered from left to right as ammonium nitrate, TNT, DNT, PETN, RDX, potassium nitrate, and urea nitrate.

Our preliminary analysis results also show that the accuracy decreases when the least squares analyses use a database of all eight substances compared to using a database of only four substances. This may be due to the increased possibilities to fit both real spectra with large variations and background noise to the spectra in the larger database. Further

4 UV Raman measurements

In order to be eye safe, the Raman system would need to use UV laser, since UV light is much less hazardous to the eye than visible light. The use of invisible UV light for detection would also make it possible to perform detection without drawing attention from the public, and even without anyone knowing.

4.1 Experimental

In order to investigate how the Raman signal intensity changes with the wavelength of irradiation, measurements have been made using a tunable band pass filter to suppress scattered laser light, enabling measurements in the interval 320-360 nm. The transmission bandwidth of the filter was about 16 nm, allowing the spectral interval of 900-1800 cm^{-1} to be measured, where the most important Raman peaks of the investigated substances are found. At 355 nm, measurements have also been made with a sharp-edge long pass filter, with which a larger part of the spectra, 500-4000 cm^{-1}, was measured. For comparison, reference Raman spectra have been measured with a standard analytical instrument, an FTIR/Raman spectrometer operating at 1064 nm.

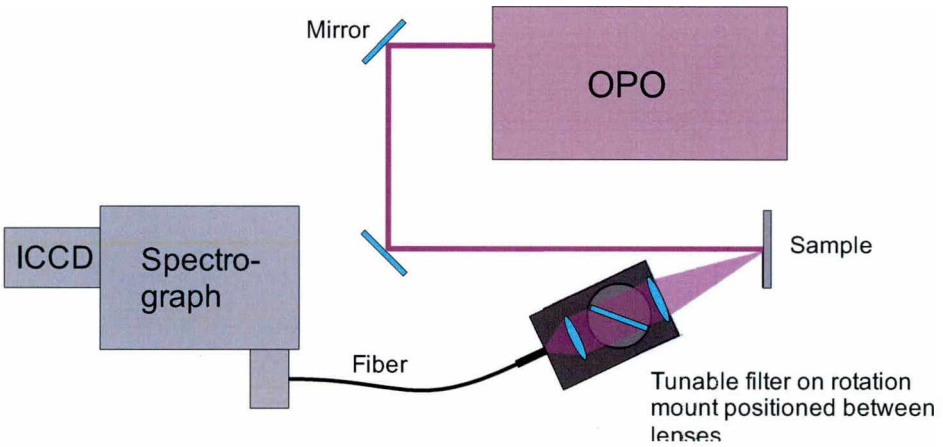

Figure 11. Schematic picture of the experimental setup.

A schematic picture of the experimental setup is shown in Figure 11. A tunable, Nd:YAG pumped OPO laser (Ekspla, NT343/3/UVE) with a pulse length of 5.6 ns and 10 Hz repetition frequency was used to illuminate a sample. The laser beam was directed towards the sample with two UV mirrors, giving a 150 cm beam path from the laser to the sample. Scattered light from the sample was collected and collimated with a 250 mm UVFS lens in front of the tunable filter (Semrock, VersaChrome TBP01-380/16-25x36). This is a tunable notch filter, where the band pass depends on the angle of incident light on the filter. The filter was placed in a rotational stage in order to change the incident angle and thereby the band pass, as the wavelength of the laser was changed. Behind the filter, the transmitted light was focused onto a round-to-slit optical fiber (Art Photonics FB-50xVIS50-S) by a 50 mm UVFS lens. The fiber end, the lenses and the filter were enclosed in a box made of black, mat foil, to prevent scattered light, reflected on the surroundings, from passing behind the filter. The optical fiber was connected to an f#-matcher (Andor, PR-ASM-0039) at the input of the spectrometer (Andor, Shamrock 500). The spectrometer has an integrated filter holder, where a 355 nm laser line sharp-edge long pass filter (Semrock, LP03-532RS-25) was placed during the 355 nm measurements. For the measurements with the tunable filter, the spectrometer was using a 2400 lines/mm grating, while a 600 lines/mm grating was used for the 355 nm measurements. The spectrometer slit entrance

was 100 µm. A gated ICCD camera (Andor, iStar 340T-18U-03) with 1300x512 active pixels, each 13x13 µm in size, registered the signal at the spectrometer output. The camera was cooled to -30°C in order to decrease thermal noise. The camera gain was set to 2000, corresponding to a 500 times signal enhancement. Every measurement was a sum of 1000 accumulations, i.e. 100 seconds measurements.

The sample substances were Teflon (used as a reference), 2,4,6-trinitrotouluene (TNT), potassium chloride (PC), ammonium nitrate (AN), urea nitrate (UN) and hexogen (RDX). The samples were tablets, 2-3 mm thick and 10 mm in diameter. They were placed in holes with the same diameter in aluminum plates during the measurements. The laser wavelength was stepped from 320 to 360 nm in 4 nm steps (together with the tunable filter), and Raman spectra were measured from every substance, as well as the pulse energy of the laser, at each laser wavelength before the wavelength was changed. The TNT and RDX samples, which were apparently affected by the illumination, becoming somewhat colored, were replaced after every measurement. For the other substances no change was observed, neither visible effects in the samples nor in the detected intensity of the Raman signal.

4.2 Results and discussion

Figure 12 shows Raman spectra of all substances measured at 355 nm. The quality of the spectra can be compared to that of the reference spectra, measured at 1064 nm, as shown in Figure 13. All the main peaks from the reference spectra are clearly displayed in the 355 nm measurements, though with somewhat lower resolution. The exception is TNT, for which none of the peaks is revealed in the 355 nm spectrum (some unidentified signal is seen around and below 800 cm^{-1} though). The reason for this is possibly light absorption from the sample, or sample dissociation. For some of the substances, the relative peak intensities differ between the 1064 and the 355 spectra. This could indicate a slight resonance enhancement for some of the peaks. All the 355 nm spectra (except for TNT) show a slope (to different extent) that grows higher towards higher wave numbers. This probably originates from laser stray light, or from fluorescence.

Raman spectra measured at 355 nm, but with the tunable filter, and therefore showing a narrower spectral interval, are shown in Figure 14. The strongest Raman line in each spectrum has been marked in the figure. The magnitudes of these peaks have been plotted as a function of irradiation wavelength in Figure 15 and Figure 16, where Figure 16 shows the same information as Figure 15, but with a logarithmic scale. In these figures, the laser pulse energy is also plotted as a function of wavelength. The drop in laser pulse energy at 355 nm is reflected in the drop in measured Raman signal for the different substances. It can be seen that the Raman signal from PC follows the variation of the energy quite well. However, the Raman signal from AN, UN and RDX, which is high compared to that of the other substances at 355 nm, decrease considerably towards shorter wavelengths.

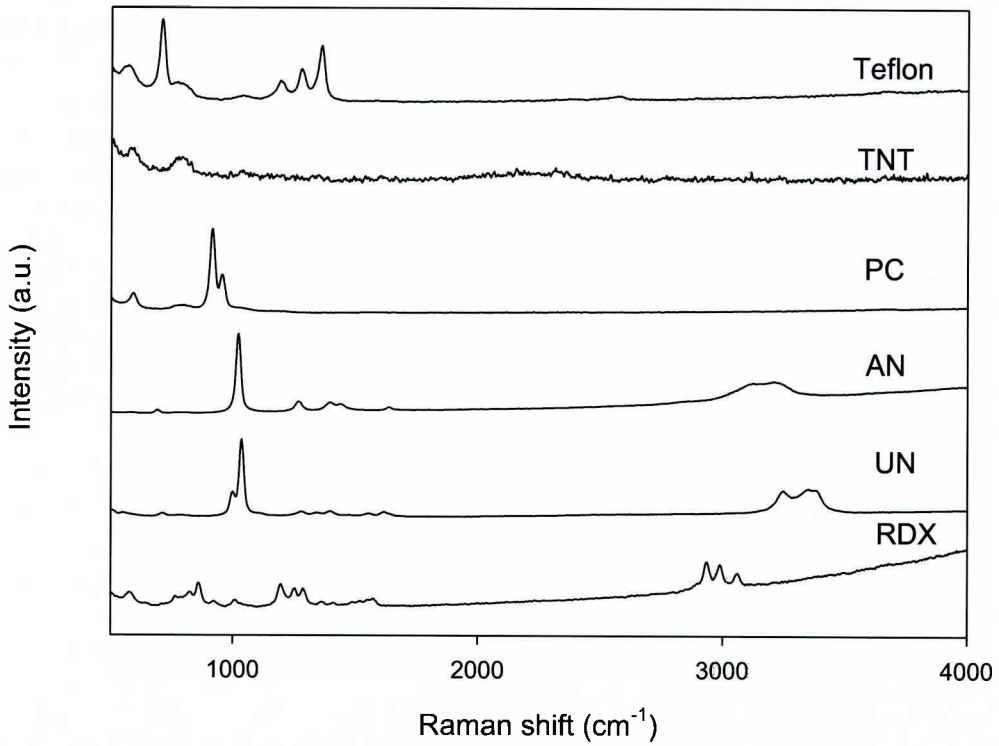

Figure 12. Raman spectra measured at an irradiation wavelength of 355 nm.

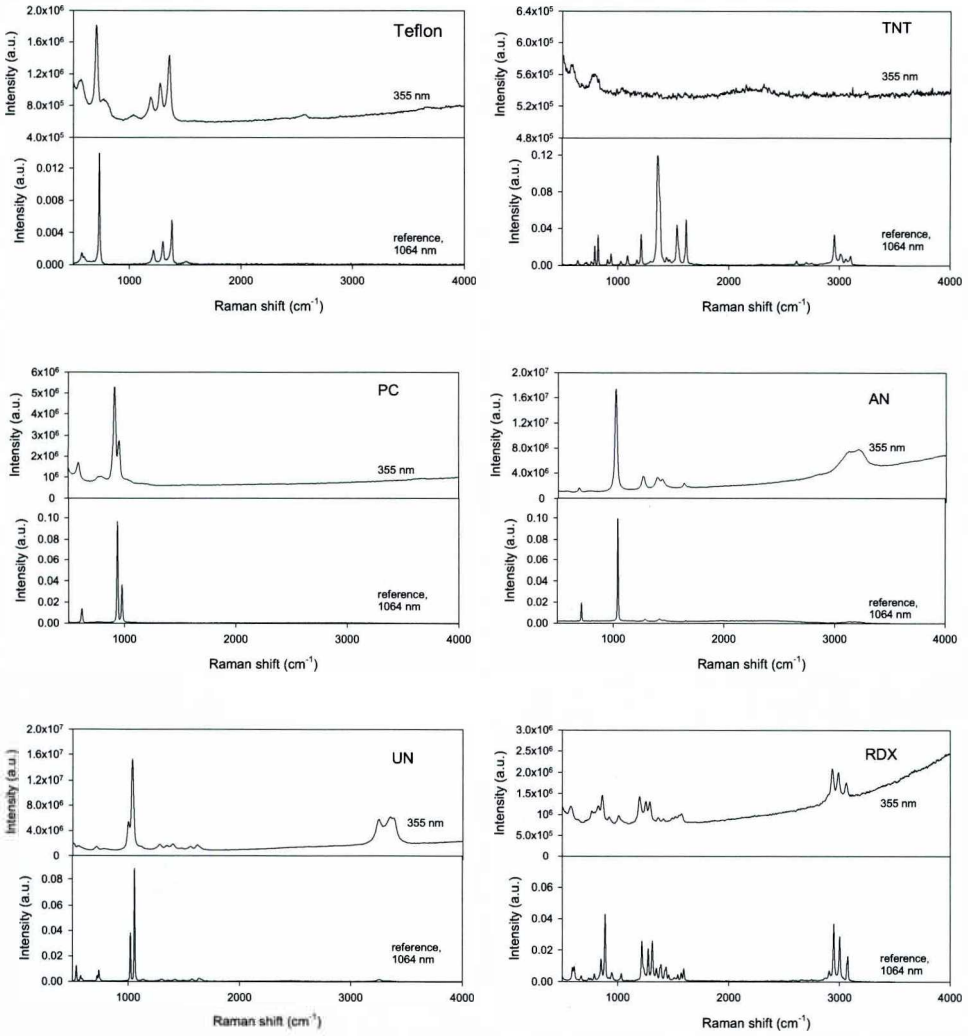

Figure 13. Raman spectra measured at an irradiation wavelength of 355 nm, (above in each figure) and reference Raman spectra measured with a standard analytical instrument operating at 1064 nm (below in each figure).

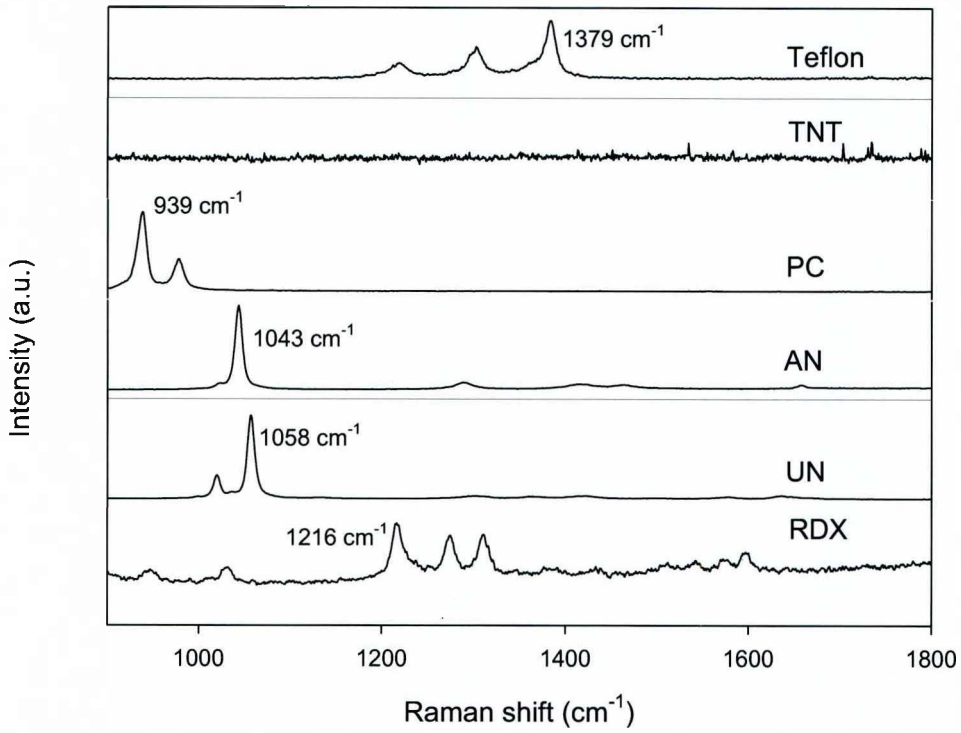

Figure 14. Raman spectra measured at an irradiation wavelength of 355 nm, using the tunable filter. For the marked peaks, the magnitude is evaluated for irradiation wavelengths in the interval of 320-360 nm, and is shown in Figure 15 and Figure 16.

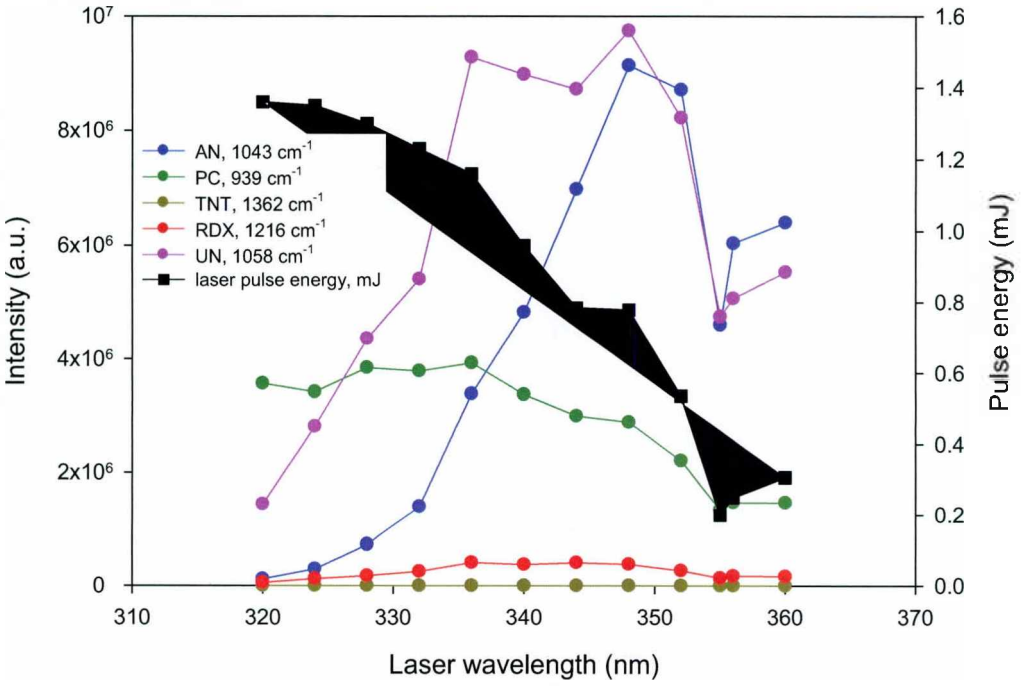

Figure 15. Measured Raman signal intensity and laser pulse energy as a function of irradiation wavelength.

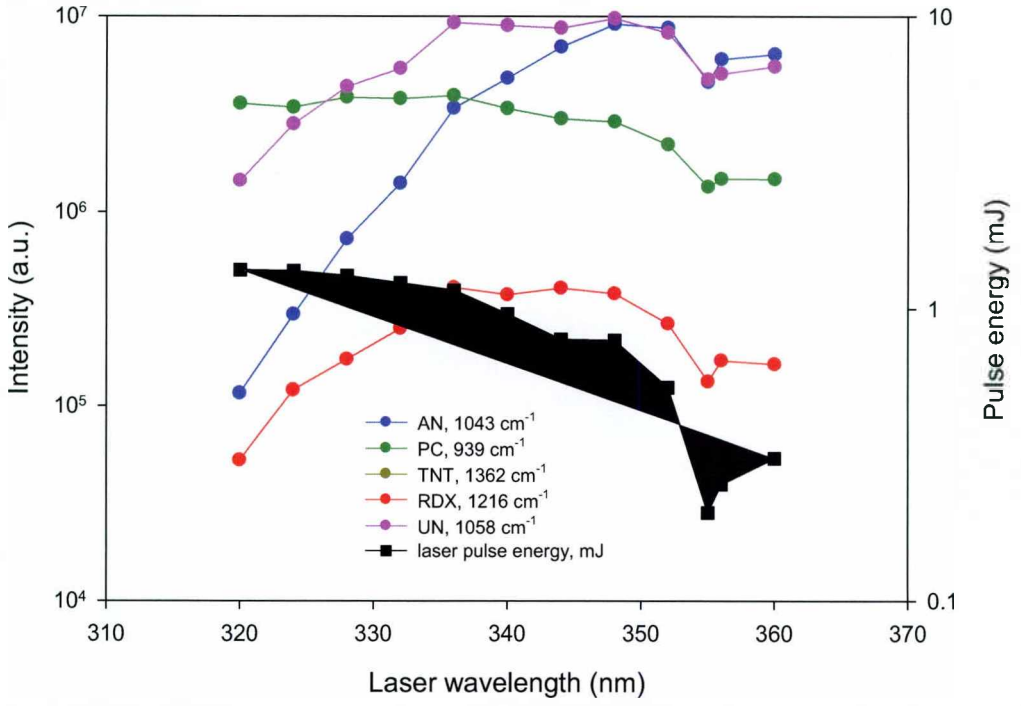

Figure 16. Measured Raman signal intensity and laser pulse energy as a function of irradiation wavelength, logarithmic scale. TNT is out of range and cannot be displayed here

5 Laser study for 355 nm wavelength

In order to make the detection system eye safe, skin safe and invisible, the wavelength of the laser must be outside the visible spectrum. This together with the $1/\lambda^4$ dependence of the Raman cross section a laser with a wavelength in the UV-range is a good choice. In this project a wavelength of 355 nm is chosen since a small compact solid state laser can be made at this wavelength. In this study, Raman spectra for different substances at 355 nm using lasers with different repetition frequencies and pulse energies have been measured.

5.1 Experimental setup

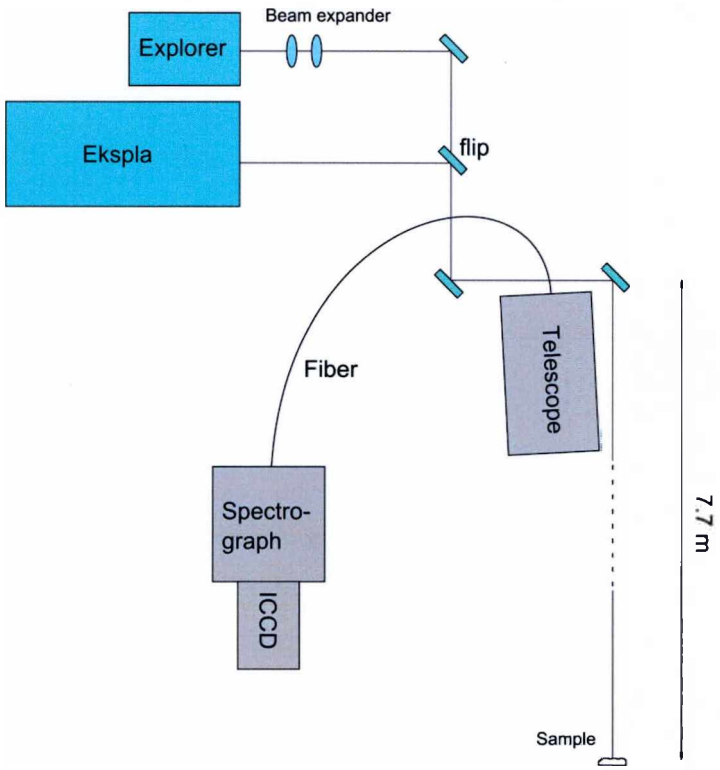

Figure 17 Sketch of experimental setup.

The lasers used were; a) an Ekspla NL303G with 4.6 ns pulse length (fwhm), 20 Hz repetition frequency and 138 mJ pulse energy at 355 nm and b) an Explorer 355 nm DPSS laser from Spectra Physics with a repetition of 20-50 kHz and a pulse length of less than 15 ns (fwhm). The average power of the Explorer laser at 50 kHz is 300 mW which gives a pulse energy of 6 μJ, but could be set to different values by changing the current of the laser (4-6.5 A).

The laser beams were directed towards the target using 355 nm YAG-coated mirrors and flip holders, see Figure 17. The stand-off distance to the target was 7.7 m. The samples (TNT, RDX, C4, Comp B, PETN based plastic explosives, DNT and PETN) were shaped into 10 mm diameter tablets with a thickness of 2-3 mm and a weight of about 300 μg. The samples were placed in a sample holder made of aluminum at the target area so that the samples were placed at exactly the same place every time. The average power of the laser was measured through a hole in an aluminum plate (same size and place as the targets) before each measurement.

The scattered light was collected with a 6" telescope (Celestron C6-A-XLT) from 7.7 m distance. The collected light was focused into a round to slit optical fiber (Art Photonics FB-50xUV-VIS50-S) using a -100 mm and a 30 mm UVFS lens. Between the lenses a Semrock 355 nm long pass filter was used to block the laser line. The other end of the optical fiber is connected to an f-number matcher (Andor SR-ASM-0018) at the input of the spectrometer (Andor Shamrock 303i-A). The spectrometer uses a 600 groves/mm grating and a slit width of 100 µm. A gated ICCD-camera (Andor iStar DH740I-18F-03) was connected to the output and cooled to -10 °C.

5.2 Results and discussions

The gate width of the camera was set to 20 ns and the optimal delay was determined by monitoring the PTFE Raman signal and choose the delay that gave the strongest Raman signal.

For TNT the Ekspla laser was set to 270 mW power and the Explorer laser to 220 mW at 20, 30, 40 and 50 kHz. The gain of the camera was 250 and 300 measurements were made with an integration time of 1 s. The samples were darkened during the measurements and therefore a new tablet was used after each 300 measurements. After the measurements the TNT-samples were analyzed using GS-MS for traces that could indicate that the TNT was not decomposed. The result from the analysis did not show anything else but TNT, which is an indication that the blackening is not a destructive process.

The measurements with the Ekspla laser show strange peaks that do not coincide with the reference spectrum for TNT. These peaks originate from the sample holder itself and are only visible when the Raman spectrum from TNT is very weak.

In Figure 18 the result from TNT can be found. All spectra are an average of over 300 measurements. Note the peaks at 1550 cm^{-1} and 2330 cm^{-1} which are related to oxygen and nitrogen. The strong Raman line of TNT at 1365 cm^{-1} can be found for spectra measured with the Explorer and the reference spectrum measured at 1064 nm. For the Ekspla laser this line is almost not notable.

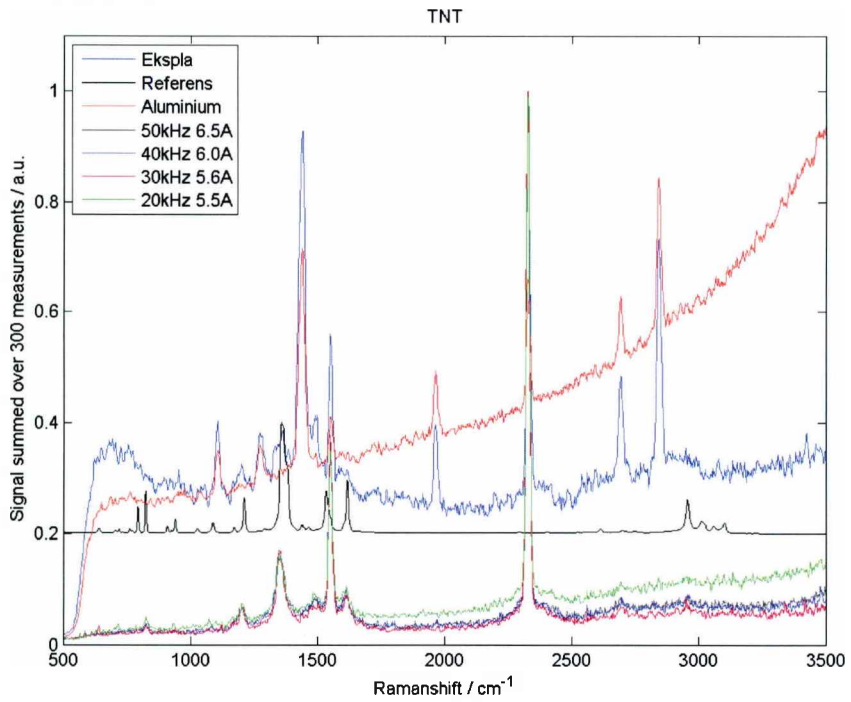

Figure 18 Raman spectra from TNT.

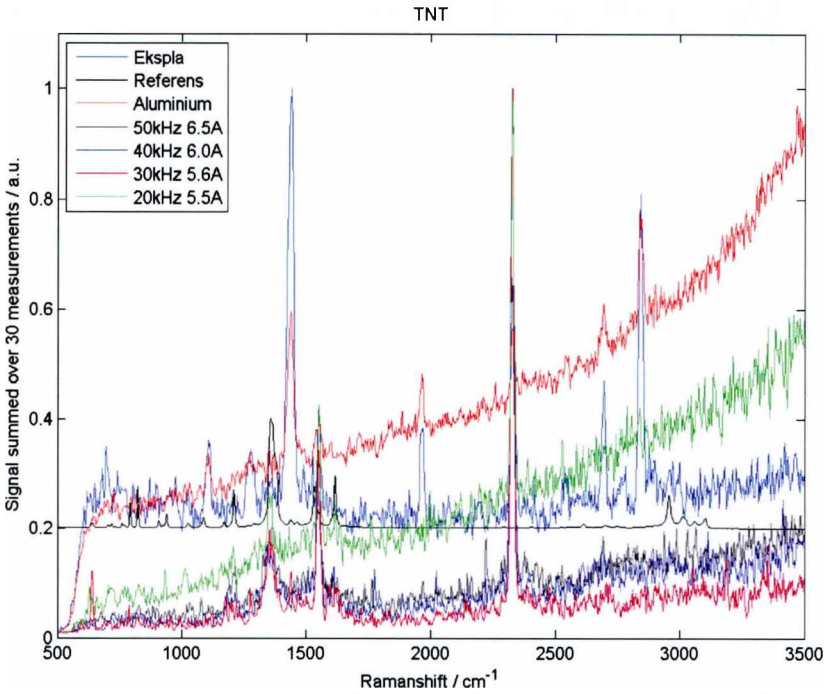

Figure 19 Raman spectra from TNT.

Figure 19 shows spectra that are a summation of the first 30 measurements. There is no obvious difference compared to the other spectra in figure 9 except for the worse signal to noise ratio.

For measurements on ammonium nitrate, the Explorer laser was used at 20 kHz (285 mW) and 50 kHz (230 mW). The Ekspla laser was set to 250 mW. All measurements were performed with 50 gain and 100 measurements with an exposure time of 1 s. Figure 20 shows an average of all 100 measurements and is very good for all the different lasers.

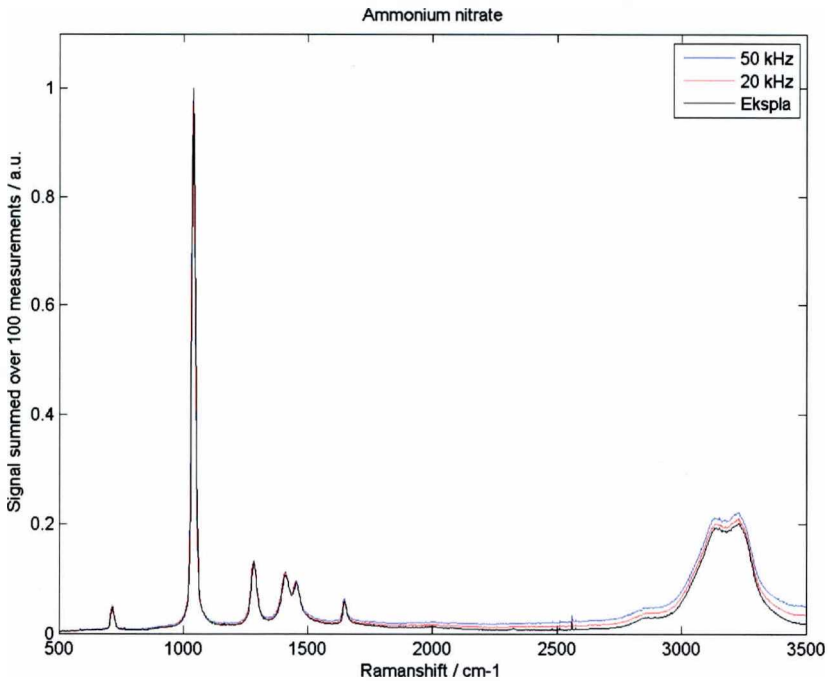

Figure 20 Raman spectra from ammonium nitrate.

The measurements on RDX were made with the Explorer laser at 20 kHz (285 mW) and 50 kHz (230 mW). The Ekspla laser was set to 280 mW. The gain was set to 100 and 100 measurements were carried out with 1 s exposure time. Figure 21 shows a summation over all measurements.

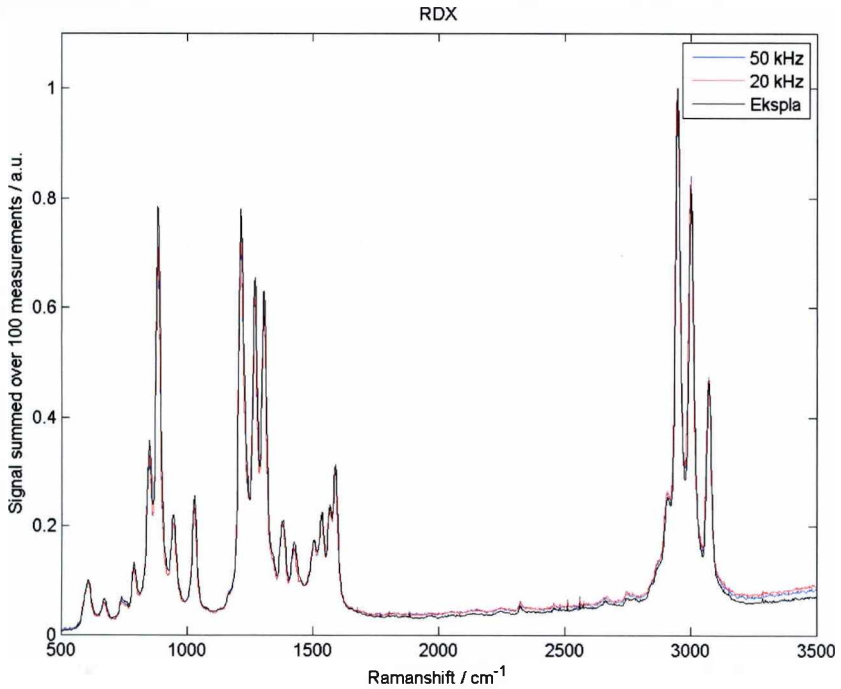

Figure 21 Raman spectra from RDX.

For measurements on PETN the Explorer laser was used at 20 kHz (285 mW) and 50 kHz (230 mW). The Ekspla laser was set to 265 mW. The gain was set to 50 and 10 measurement were made with an exposure time of 1 s. The spectra show very good results, see Figure 22.

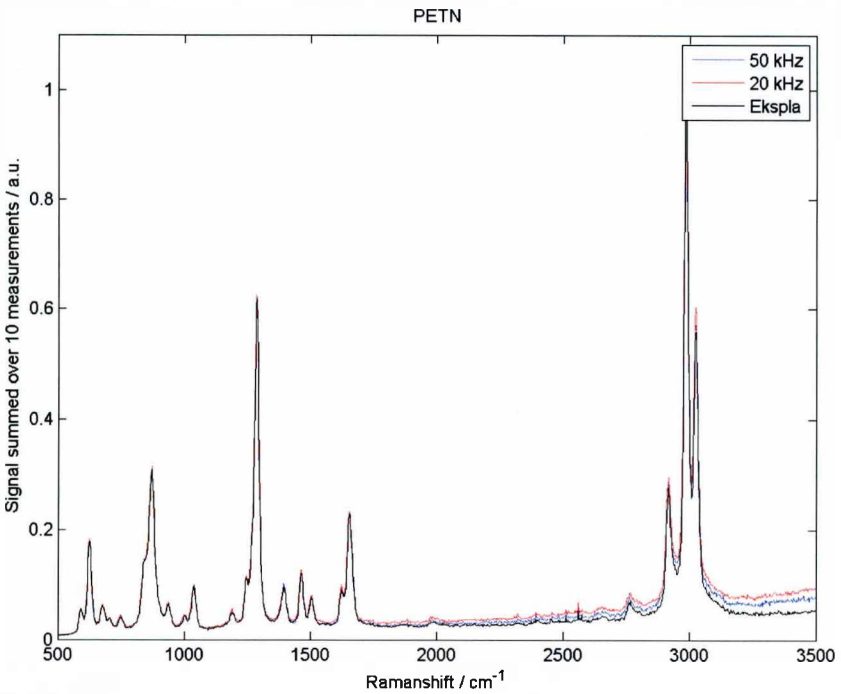

Figure 22 Raman spectra from PETN.

The measurements on Comp B were made with the Explorer laser at 20 kHz (285 mW) and 50 kHz (230 mW). The Ekspla laser was set to 260 mW. The gain was set to 250 and 60 measurements with an exposure time of 1 s were conducted, see Figure 23. All samples became brownish as can be seen in Figure 24. The result is similar to those measured on TNT, i.e. only weak peaks can be found and for the Ekspla laser peaks from the background can be seen.

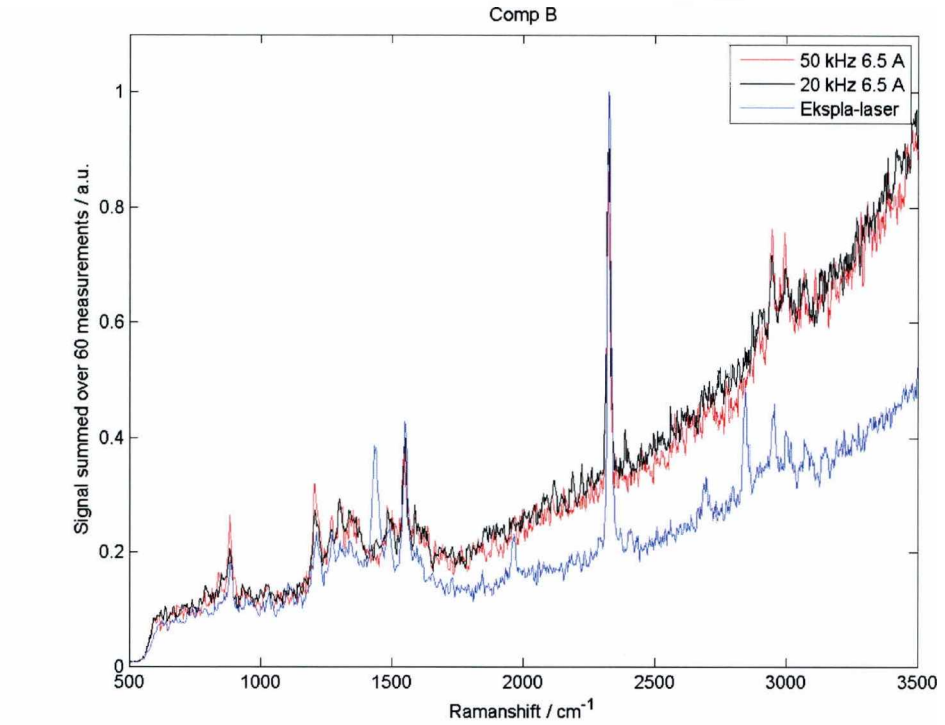

Figure 23 Raman spectra from Comp B.

Explorer 50 kHz and 230 mW.	Explorer 20 kHz and 285 mW.	Ekspla 260 mW.

Figure 24 Pictures of Comp B after 60 s of illumination with 355 nm laser.

Figure 24 shows pictures of Comp B after illumination with different lasers. The sample darkens in all cases and for the Explorer laser holes are visible.

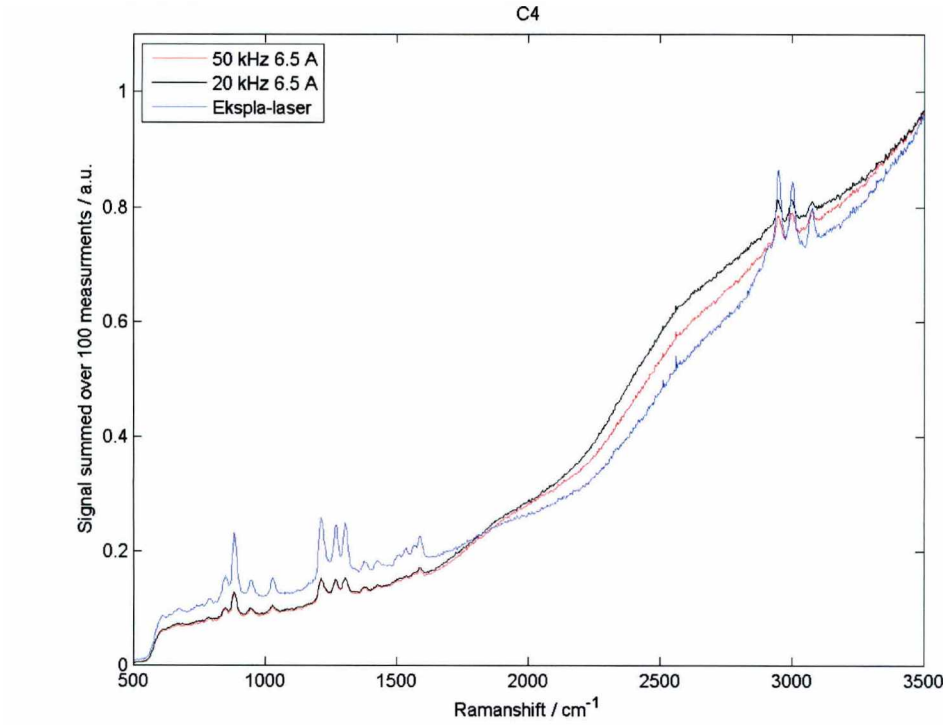

Figure 25 Raman spectra from C4.

Measurements on C4 were made with the Explorer laser at 20 kHz (285 mW) and 50 kHz (230 mW). The Ekspla laser was set to 260 mW. On the samples a weak discoloration was seen after the measurements, thus the sample was changed after each series. For all measurements a gain of 50 was used and 100 measurements with 1 s acquisition time were made. The result shows strong fluorescence from measurements made with all different lasers but the Raman spectra are still visible in all spectra, see Figure 25.

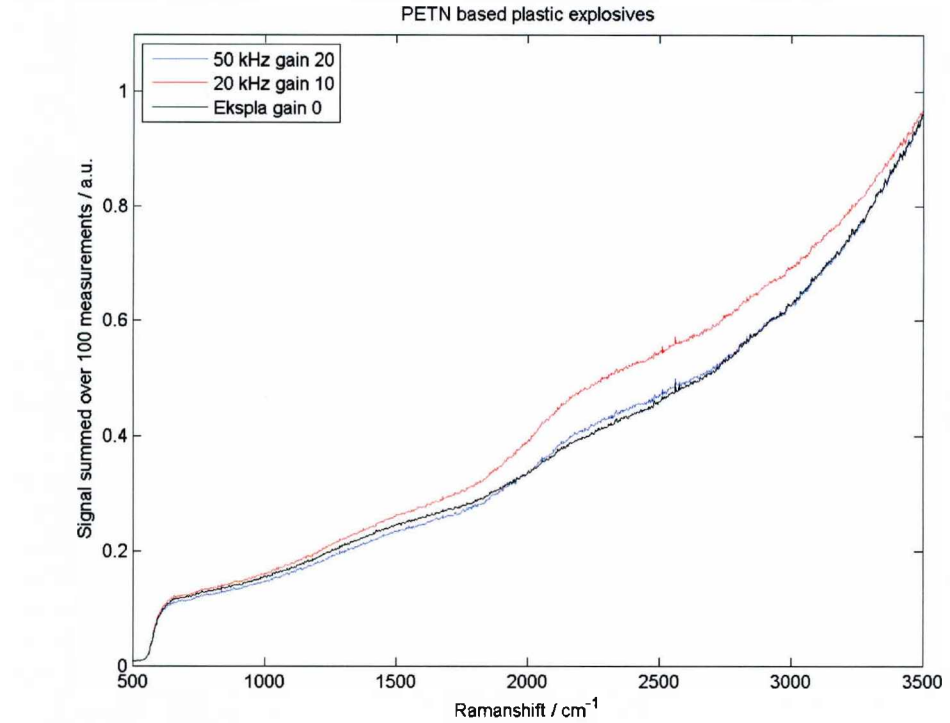

Figure 26 Raman spectra from PETN based plastic explosives.

For the measurements on PETN based plastic explosives the Explorer laser at 20 kHz (285 mW) and 50 kHz (230 mW) was used. The Ekspla laser was set to 250 mW. The substance gives very high fluorescence and therefore the gain was set individually for each laser to not saturate the camera. For the 20 kHz, 50 kHz and Ekspla laser, the gain was set to 10, 20 and 0. For each target 100 measurements with an exposure time of 1 s were recorded. The fluorescence decreased after a few measurements for each sample and the sample also became a little brownish. An average over all measurements for each laser can be seen in Figure 26. The Raman spectra cannot be seen due to too strong fluorescence from the sample.

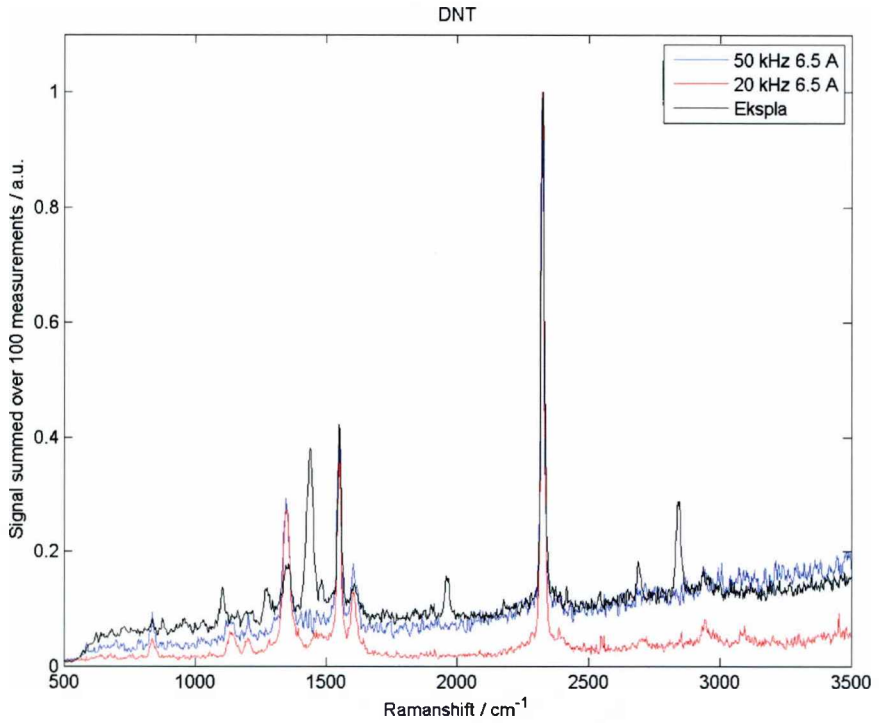

Figure 27 Raman spectra from DNT.

The measurements on DNT were made with the Explorer laser at 20 kHz (285 mW) and 50 kHz (230 mW). The Ekspla laser was set to 250 mW. The gain was set to 250 and 100 measurements with a 1 s exposure time were performed. The samples showed a yellowish melted hole after each series and therefore the sample was replaced after each new series. The result shown in Figure 27 is a summary of all measurements for each substance. Weak Raman signals can be seen with each laser. The Explorer laser gives the strongest Raman signal, at 20 kHz frequency it gives a little stronger signal than at 50 kHz. Note the oxygen and nitrogen peaks at 1550 cm^{-1} and 2330 cm^{-1}. Again, the background peaks can be seen with the Ekpla laser.

For TNT and similar substances (DNT and Comp B), the Raman signal is very weak at measurements made with a 355 nm laser. Other groups have reported good results in the UV region for these substances. Analyses made from TNT samples after measurement show no decomposition of TNT into other substances and therefore it is likely that no chemical process has taken place. Measurements on ammonium nitrate, RDX and PETN show very good Raman spectra at 355 nm with no particular difference irrespective of laser used. C4 and PETN based plastic explosives generate strong fluorescence during illumination but C4 shows a detectable Raman spectra.

6 Conclusions

A graphical user interface (GUI) has been manufactured in order to make the system easy to control and maneuver. The GUI has one main page that is used for normal usage and subpages for advanced settings. Initial testing of the GUI has been made and almost the whole system can be controlled by this.

In order to identify the targets, least squares and correlation methods are being evaluated. A first step has been to reduce the number of Raman shifts to measure at by feature selection. Preliminary results shows that when using least square fitting the number of shifts can be decreased to 8-10 shifts if sulfur, ammonium nitrate, DNT and TNT is used as targets. Also least square fittings show worse result when increasing the number of targets to eight. This is probably due to the fact that it is more likely to find a combination of several reference spectra to match the measured spectrum than if there are only a few reference spectra.

Raman spectra from PTFE, TNT, potassium chlorate, ammonium nitrate, urea nitrate and RDX have been recorded at 355 nm laser wavelengths. All spectra show clear spectral information except TNT. The reason for this is probably sample dissociation or light absorption in the sample. The relative intensity between the peaks in the spectrum differs from what is measured at 1064 nm. This could indicate slight resonance enhancement for some of the peaks. Using a tunable OPO-laser and a tunable notch filter Raman spectra has been measured in the 320-360 nm laser wavelength range. Results show that the intensity of the measured Raman spectra from potassium chlorate follows the laser intensity as expected, while for ammonium nitrate, urea nitrate and RDX the signal decreases considerably towards shorter wavelengths.

In order to investigate if there are any significant differences between high- and low-repetition frequency lasers, Raman measurements have been made on TNT, DNT, Comp B, RDX, C4, PETN, PETN based plastic explosives and ammonium nitrate using 20 Hz, 20 kHz and 50 kHz lasers all with similar laser power. The results are essentially the same for all laser types. For TNT, DNT and Comp B the measured Raman spectra are very weak for all types of laser. For these substances the high repetition frequency might give a little better result but this is inconclusive and should be investigated further with a laser that can be set arbitrarily in the whole repetition frequency range. Such a laser is not easy to find and therefore these measurement are difficult to accomplish.

References

1. Pettersson, A., et al., *Near Real-Time Standoff Detection of Explosives in a Realistic Outdoor Environments at 55 m Distance*. Propellants Explos. Pyrotech, **2009**. 34: p. 297-306.
2. Pettersson, A., et al., *Standoff Detection of Explosives at Ranges up to 470 m.* To be published.
3. Nordberg, M. Akke, F (Portendo) and Pettersson, A. *Detection limits of stand-off spontaneous Raman scattering*. **2009** (FOI-R—2794—SE).
4. Ehlerding, A., et al., *Stand-off detection of vapor phase explosives by resonance enhanced Raman spectroscopy*. Proc. of SPIE **2010**, 7835
5. Nordberg, M., et al., *Detection of Explosives Particles by Imaging Raman Spectroscopy*. **2008** (FOI-RH-8300-SE).
6. Östmark, H., et al., *Stand-off Detection of Explosives Particles by Multispectral Imaging Raman Spectroscopy.* To be published in Applied Optics
7. Nordberg, M., et al., *Stand-off Detection of Explosive Particles by Imaging Raman Spectroscopy*. Proc. of SPIE **2011**, 8017

FOI, Swedish Defence Research Agency, is a mainly assignment-funded agency under the Ministry of Defence. The core activities are research, method and technology development, as well as studies conducted in the interests of Swedish defence and the safety and security of society. The organisation employs approximately 1000 personnel of whom about 800 are scientists. This makes FOI Sweden's largest research institute. FOI gives its customers access to leading-edge expertise in a large number of fields such as security policy studies, defence and security related analyses, the assessment of various types of threat, systems for control and management of crises, protection against and management of hazardous substances, IT security and the potential offered by new sensors.

FOI
Defence Research Agency
Defence & Security, Systems and Technology
SE-164 90 Stockholm

Phone: +46 8 555 030 00
Fax: +46 8 555 031 00

www.foi.se